# Modeling the electrostatic component of toner adhesion and detachment

*Brandon A. Kemp; Arkansas State University; Jonesboro, Arkansas/USA*

## Abstract

*In this paper, we explore both the physical and mathematical models of electrostatic adhesion. Addressed topics include, review of the dipole and analytical field expansion models of adhesion, addition of an applied field in the analytical model for electrostatic detachment, parametric studies of adhesion and detachment, and analysis of the model for non-uniform particle charge distribution.*

## Introduction

Toner adhesion affects development, transfer, and cleaning, and thus, it a significant issue in electrophotography [1]. Discrepancies between predictions and measurements have ignited a debate over toner particle adhesion. An understanding of both electrostatic and non-electrostatic components of adhesion significantly benefits the development of electrophotographic printing systems and also have implications to other powder processing industries.

Chemically processed toners used in electrophotographic printing are fairly uniform micro-particles with repeatable and predictable ability to become electrostatically charged. Present toner particles made for office printing systems are generally 5 to 7 $\mu m$ in diameter, composed of a resistive polymer base and an outer coating of small silica additives to reduce cohesion and improve system performance. Significant controversy has arisen as to the relative magnitude of the electrostatic forces as compared to the Van der Waals or dispersive forces also acting on the particles. Measurement of adhesion in toner has taken multiple forms, including ultracentrifuge, electrostatic removal, microcantilever testing, and blow-off devices [2]. All of these methods have indicated forces on the order of 10x what would be predicted from a simple Coulombic attraction model to a substrate [3]. Recent experimental studies aim to understand the electrostatic and non-electrostatic mechanisms of adhesion as well as the relationship between the mechanisms [2, 4, 5]. In this correspondence, we further explore both the physical and mathematical models of electrostatic adhesion.

## Electrostatic Force Models

In toner transfer, particle detachment is accomplished primarily by electrostatic forces. The substrates considered herein are intermediate transfer belts. Intermediate transfer belts generally have complex charge transport mechanisms, but for practical purposes, their electrical properties can be summarized by bulk electrical characterization measurements [6]. These belts are electrically semi-insulating, but behave as image planes as long as the time between toner attachment and detachment is longer than the electrical relaxation time. The simple Coulombic attraction model assumes a uniform charge distribution on a single spherical particle with unity dielectric constant resting on an image plane. In this situation, the adhesion force is given by

$$F_0 = \frac{Q^2}{16\pi\varepsilon_0 R^2} \tag{1}$$

where $Q$ is the total charge, $R$ is the particle radius, and $\varepsilon_0 = 8.85 \cdot 10^{-12}\ F/m$ is the permittivity of air. Several modifications to this model have been made which increase the predicted electrostatic adhesion. First, it has long been suspected that non-uniform charge distribution on a toner particle increases adhesion force [7]. Second, the effect of dielectric polarization has been studied analytically [8], and the inclusion of a dielectric constant of $\varepsilon = 3$ gives about 50 % enhancement over $F_0$ for a single spherical particle [9]. Third, considering multiple particles in the attraction model can give a 5 to 7x enhancement over $F_0$. Finally, the proximity force yields an enhancement of $1 + 4/\pi \approx 2$x as compared to $F_0$ and is due to the discrete nature of charge [10]. Recently, it was shown that inclusion of dielectric polarization, multiple particles, and non-uniform charge together in a single analytical model can account for nearly a 10x increase over $F_0$ [9]. These results explain how electrostatic interactions between between multiple, non-uniformly charged dielectric micro particles and a substrate can explain the order-of-magnitude difference between measurement and theory [11]. In this section, we explore both the full analytical field expansion model and the dipole approximation [11, 12].

### *Dipole Model*

For polarizable particles, interactions between the monopole and dipole response is often modeled by

$$F_d = -\alpha\frac{q^2}{16\pi\varepsilon_0 R^2} + \beta q E_0 - \gamma\pi\varepsilon_0 R^2 E_0^2, \tag{2}$$

where the dimensionless coefficients $\alpha$, $\beta$, and $\gamma$ are often used to fit experimental data [13]. Using a dipole approximation, the coefficients in Eq. (2) can be approximated by [12]

$$\alpha \approx 1 + \frac{1}{2}\xi + \frac{3}{32}\xi^2 \tag{3a}$$

$$\beta \approx 1 + \frac{1}{2}\xi + \frac{3}{16}\xi^2 \tag{3b}$$

$$\gamma \approx \frac{3}{2}\xi^2, \tag{3c}$$

where $\xi = (\varepsilon - 1)/(\varepsilon + 2)$ is the Clausius-Mossotti factor. The dipole approximation is more accurate when either the particle is weakly polarizable (i.e. $\varepsilon$ is close to one) or when the distance between the particle and the substrate is large. Because of this, the model may be useful, but the values may significantly differ from

 

the exact solution in adhesion and detachment studies. While this model is approximate, the analytical model previously presented in Refs. [11, 9] is an exact solution for the force on a charged spherical particle near an image plane as the number of spherical modes $N$ approaches infinity. In other words, by increasing the number of terms in the summation, one can achieve a desired precision. The analytical model has been expanded to include a $z$-directed applied electric field $E_0$. This uniform field has been added by expansion in the spherical basis and can be used in detachment studies [12]. Such parametric studies reveal interesting physics of particle adhesion and detachment.

### *Analytical Expansion Model*

The exact model of multiple spherical particles in an applied field is obtained by application of the multi-scattering technique to electric fields. The surface charge density on particle $j$ is expanded in the spherical basis and defined by the coefficients $\alpha_{nm}^{(j)}$,

$$\rho_s^{(j)}(\theta,\phi) = \sum_{n=0}^{N}\sum_{m=-n}^{n} \alpha_{nm}^{(j)} P_n^{|m|}(\cos\theta_j) e^{im\phi_j}. \tag{4}$$

In previous studies [9, 11, 12], $\phi$ symmetry of the surface charge $\rho_s$ limited the nonzero values of the coefficient to $\alpha_{n0}$. Here, this restriction is lifted such that, in general, $\alpha_{nm}$ are all nonzero coefficients determined by mode matching with the input charge distribution. Also, a uniform applied electric field $E_0$ is given by the potential $\psi_0(r_j,\theta_j,\phi_j) \equiv -E_0 z$ so that

$$\psi_0(r,\theta,\phi) = \sum_{n=0}^{N}\sum_{m=-n}^{n} \gamma_{nm}^{(j)} r_j^n P_n^{|m|}(\cos\theta_j) e^{im\phi_j}, \tag{5}$$

where $\gamma_{nm}^{(j)} = 0$ except for $\gamma_{10}^{(j)} = -E_0$. The potential internal and external to particle $j$ is expanded in the spherical basis and are given by

$$\psi^{int}(r,\theta,\phi) = \sum_{n=0}^{N}\sum_{m=-n}^{n} A_{nm}^{(j)} r_j^n P_n^{|m|}(\cos\theta_j) e^{im\phi_j} \tag{6a}$$

$$\psi^{ext}(r,\theta,\phi) = \sum_{n=0}^{N}\sum_{m=-n}^{n} \left[B_{nm}^{(j)} r_j^{-(n+1)} + W_{nm}^{(j)} r_j^n\right] \times P_n^{|m|}(\cos\theta_j) e^{im\phi_j}. \tag{6b}$$

The coefficients give the magnitudes of the spherical modes internal to particle $j$ ($A_{nm}^{(j)}$), external to the $j^{th}$ particle due to scattering from particle $j$ ($B_{nm}^{(j)}$), and external to the $j^{th}$ particle due to all other sources besides particle $j$ ($W_{nm}^{(j)}$). The mode coefficient $W_{nm}^{(j)} = \sum_k L_{nm}^{(jk)} + \gamma_{nm}^{(j)}$, therefore, includes scattering from all other particles, all particle images, and the applied electric field. A unique solution is obtained by invoking a translational theorem [14] and the boundary conditions at the surface of each particle. Details of the electric field expressions, boundary conditions, and solutions for the expansion coefficients have been previously reported [9, 11].

The total force on each particle can be obtained by direct application of any variation of electromagnetic force density [15] or, equivalently, by integration of the the Maxwell stress tensor [16]. The force on each particle has been shown to reduce to a simple sum of it's mode coefficients [17]. Here, we choose to numerically integrate the stress tensor to determine the force density and torque on the particle. The local electrostatic surface force density $\bar{f}(\bar{r})$ in $[N/m^2]$ at each point along the surface of a particle is determined by the divergence of the Minkowski stress tensor across the boundary [18, 19]. The local electromagnetic moment density is $\bar{\mu}(\bar{r}) = \bar{r}' \times \bar{f}(\bar{r})$ in $[N/m]$, which is computed by taking $\bar{r}'$ as the moment arm measured from the center of the particle to the surface. The total electromagnetic force $\bar{F}$ in $[N]$ and torque $\bar{\tau}$ in $[N \cdot m]$ are determined by numerical integration of the force density and moment density, respectively [20].

## Discussion of Adhesion and Detachment

In the following discussion, the exact analytical solution of electrostatic forces for spherical particles above an image plane is applied to illustrate the physics of particle adhesion and detachment in an applied field. We also include calculations of torque on a non-uniformly charged particle to aid in the discussion of the physical model which leads to a 10x enhancement in adhesion force over $F_0$ [9, 11].

### *Effect of Charge, Size, and Applied Field*

Figure 1 shows typical plots of the $z$-directed force versus applied electric field. The dependence is nonlinear [12], in agreement with experiment [13]. For the case of a weakly charged 6 $\mu m$ particle in Fig. 1 (a), the electrostatic adhesion force, that is the force holding the particle to the substrate under zero applied field, is very small. However, the maximum detachment force is also small. It reaches a maximum value of just a couple of $nN$ at about an applied field of $E_0 = 3\ V/\mu m$. This means that if the non-electrostatic component of adhesion is greater than a few $nN$'s, this particle cannot be removed by an electrostatic field. Higher applied fields actually reverse the electrostatic force and produce an attachment force. Although the dipole approximation does not fit the curve with a great deal of accuracy, the general shape of the approximate curve agrees, and we can use monopoles and dipoles to describe the physics [12]. First, the low field region of particle adhesion is dominated by Coulombic attraction between the particle charge and its image as well as the charge and image induced dipole with its dipole image. Second, under moderate field, the field induced dipole starts to cancel the charge induced dipole in the particle and image. Here, the $qE_0$ force and Coulombic attraction of the charge and its image oppose each other. As the applied field becomes larger, the field induced dipole becomes very strong and attraction between this dipole and its image causes the force to reach a maximum. Eventually, this attractive force between the field induced dipoles dominates, and the force on the particle becomes negative, attracting the particle back to the substrate. For the highly charged particle plot in Fig. 1 (b), the detachment force maximum is shifted far to the right (not shown). However, the effect of the charge and applied field induced dipole is evident. Since the adhesion force is about $F_a = 50\ nN$, it would be reasonable to assume that an applied field of $E_0 = F_a/Q = 50nN/10fC = 5V/\mu m$ would be required to just bring the electrostatic force to zero. However, the electrostatic force actually crosses zero at about $3\ V/\mu m$, indicating a detachment force for fields just greater than this value. This explains why transfer of toner occurs at fields smaller than predicted by the simpler equation $F_a/Q$, where $F_a$ is the adhesion force under zero applied field.

Figure 2 shows the relationship between the $z$-directed force

$F_z$ and the ratio of particle charge to diameter squared $(Q/D)^2$. The three cases shown are for (a) $E_0 = 0\,V/\mu m$, (b) $E_0 = 1\,V/\mu m$, and (c) $E_0 = 10\,V/\mu m$ with the uniform surface charge density held constant at $\rho_s = 1\,nC/cm^2$. In all three cases, the relationship is linear. However, the slope of the linear relationship varies according to the applied field. When the applied field is zero, and the particle becomes more attached as $Q/D$ is increased. However, when an electric field of $E_0 = 1\,V/\mu m$ is applied, the particle becomes more detached with increasing $Q/D$. The reason for this can be seen in Fig. 1 (a); moving from $E_0 = 0\,V/\mu m$ to $E_0 = 1\,V/\mu m$ crosses the horizontal axis from negative $F_z$ to positive $F_z$. Fig. 2 (c) shows that the slope once again becomes negative under the load of an increased applied electric field. The dipole approximation fails in this case as the sign $F_z$ and even the sign of the slope are incorrectly predicted to be positive.

### *Effect of Non-uniform Charge on Adhesion*

In printer systems, recharging typically occurs to the top of the particle by electrostatic breakdown of air during the passage of toner on an intermediate transfer belt through additional transfer nips. Such recharging commonly occurs post-nip due to Paschen discharge at downstream first transfer stations in color transfer systems. This results in toner which has been transferred to an intermediate belt having additional charge on the air side of the toner particles post nip. Such charge imbalances can result in a net torque on the particle causing a spherical particle to rotate so that majority of charge will be oriented closest to the image plane [21]. The chemically processed toners typically have a mean circularity very near one. In previous adhesion measurement experiments, the charge is increased by adjusting the first transfer voltage on downstream first transfer rollers [2, 4, 5]. As the analytical expansion model is applied here, a toner particle is assumed to be charged uniformly to some base charge density $\rho_0$. Additional charging occurs via a uniform ion stream which impacts only the exposed top half of the particle. Because the particle is spherical, the resulting additional charge distribution $\Delta\rho$ on the top half will be a cosine function with respect to the zenith angle. The charge on the top of the particle $(0 < \theta < \pi/2)$ is then described by

$$\rho = \rho_0 + \Delta\rho\cos(\theta) \tag{7}$$

and $\rho_0$ on the bottom of the particle $(\pi/2 < \theta < \pi)$, where $\theta$ is the usual spherical coordinate. This charge distribution is used to study force and torque on the particle as a function of rotations about the $y$-axis. This charge distribution is shown in Fig. 4 along with rotations of 0°, 45°, 135°, and 180°.

The analytical expansion model was used to compute the fields under various rotations of a single non-uniformly charged

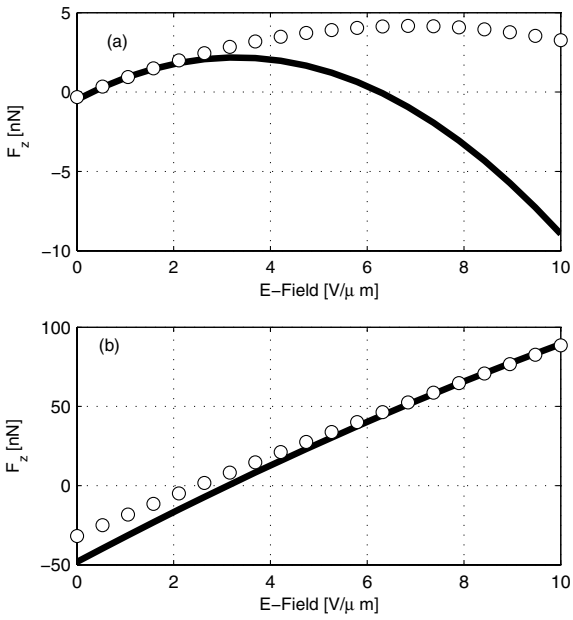


***Figure 1.*** *Electrostatic force $F_z$ on a single particle versus applied $\hat{z}$-directed electric field $E_0$ for a $6\mu m$ diameter particle with dielectric constant $\varepsilon = 4$. The charge on each particle is (a) $Q = 1\ fC$ and (b) $Q = 10\ fC$. The solid lines indicate calculations from the analytical expansion [11, 9], and the markers give calculations using Eq.* (2). *$N = 10$ modes were used in the analytical expansion.*

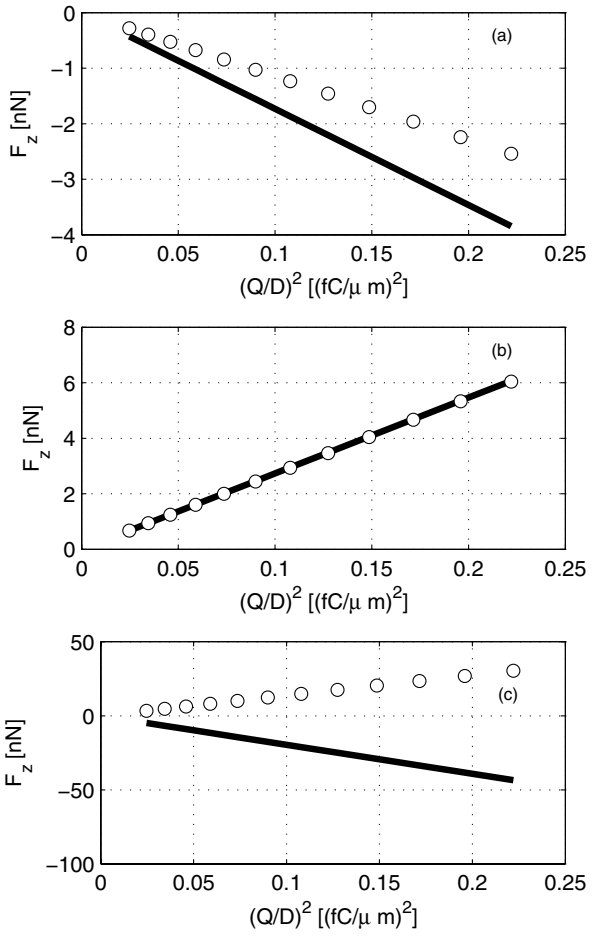


***Figure 2.*** *Electrostatic force $F_z$ on a single particle versus $(Q/D)^2$. The applied $\hat{z}$-directed electric field is (a) $E_0 = 0$, (b) $E_0 = 1\ V/\mu m$, and (c) $E_0 = 10\ V/\mu m$. The calculations are based on a constant surface charge density $\rho_s = 1\ nC/cm^2$ on particles with dielectric constant $\varepsilon = 4$ and varying diameters $D = 2R$. The solid lines indicate calculations from the analytical expansion [11, 9], and the markers give calculations using Eq.* (2). *$N = 10$ modes were used in the analytical expansion.*

particle resting on a substrate. The force and torque were computed by numerical integration using the stress tensor method as previously described [15, 16, 18, 19, 20]. Figure 4 (a) shows an example calculation of force on a particle versus rotation angle. As the particle rotates, both $F_x$ and $F_y$ remain zero, and $F_z$ increases as the bulk of the charge distribution reorients closer to the substrate. Figure 4 (b) gives the torque on the same particle. The torque is in the $y$ direction. $\tau_y$ is zero at $0^\circ$ and $180^\circ$, but reaches significant positive values for angles in between. This indicates that the particle will tend to rotate so that the majority of the charge distribution will be located at the substrate. In other words, the rotation angle $\theta = 0^\circ$ is a nonstable equilibrium, and the rotation angle $\theta = 180^\circ$ is a stable equilibrium. Under such non-uniform charge distribution, the particle will tend to reorient to the stable equilibrium state. This reorientation due to nonuniform charge has been determined to be a factor in bridging the order-of-magnitude gap between theory and measurements of particle adhesion [11].

## Conclusions

In conclusion, the analytical expansion model of charged spherical particle force has been applied to analyze the physics of electrostatic attachment and detachment in an applied static field. Although a linear response model is used for the materials, the particle-substrate interaction force is a nonlinear function of the applied field. There is a maximum detachment force which can be obtained by applying an electric field for a given adhered particle. The applied electric field required to offset the electrostatic adhesion force of a charged particle is less than the adhesion force divided by the particle charge. This is due to the effective canceling of the dipole moment by the applied field. The exact mathematical solution of a charged sphere above an image plane was used in the analysis. This analytical expansion model was used to evaluate the effectiveness of the dipole approximation. While the dipole approximation is very useful in describing the physics of particle attachment and detachment, the quantitative results are poor in many instances. Finally, we provide mathematical and physical reasoning for the nonuniform charge distribution applied to toner particles in the electrophotographic process. This model results from post-nip ionic charging at transfer. The result of this charging is a non-uniform surface charge distribution that causes the particle to reorient under an electrostatic moment. This non-uniform charge model is a factor in bridging the order-of-magnitude gap between particle adhesion theory and experiments.

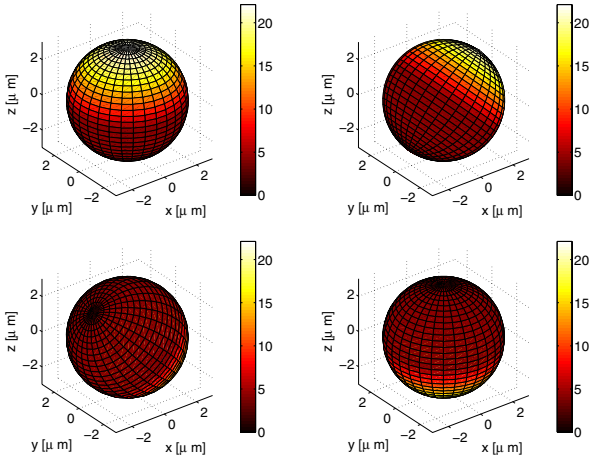


***Figure 3.*** *Surface charge density on toner particles for various rotations about the $y$-axis. The color map indicates the charge density in $nC/cm^2$. From top to bottom, the rotations are $0^\circ$, $45^\circ$, $135^\circ$, and $180^\circ$.*

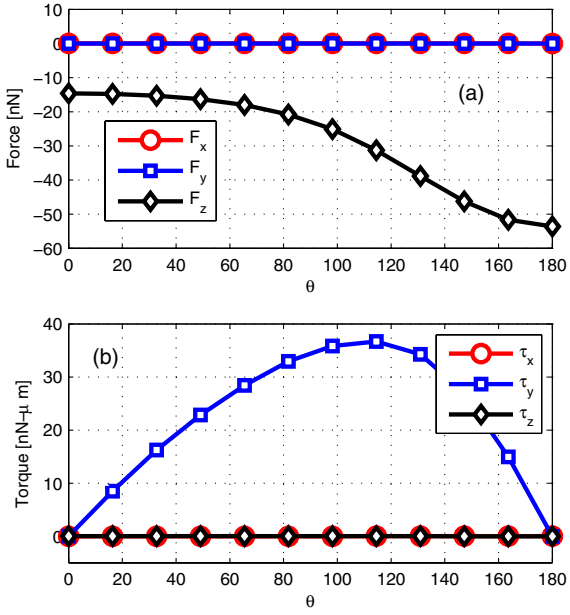


***Figure 4.*** *Surface charge density on toner particles for various rotations about the $y$-axis. The color map indicates the charge density in $nC/cm^2$. From top to bottom, the rotations are $0^\circ$, $45^\circ$, $135^\circ$, and $180^\circ$.*

## Acknowledgements

The author would like to acknowledge helpful discussions with Julie G. Whitney. This work was sponsored in part by the National Science Foundation EECS Division (award number ECCS-1150514) and by the Arkansas Science and Technology Authority for funding provided to the Center for Efficient and Sustainable Use of Resources (CESUR).

## References

[1] L. B.Schein, *Electrophotography and Development Physics*, (LaPlacian Press, CA, 1996).

[2] J. G. Whitney and B. A. Kemp, "Toner adhesion measurement", IS&T NIP **26**, 227 (2010).

[3] L. B. Schein, "Recent puzzles in electrostatics," Science **316**, 1572 (2007).

[4] J. G. Whitney, "Toner Charge and Environmental Interactions with Toner Adhesion", IS&T NIP **27**, 136 (2011).

[5] J. G. Whitney, "Toner/Transfer Member Adhesion Response to Environment-Induced Material Property Changes, and Their Impact on Transfer Fields", IS&T NIP **28**, 507 (2012).

[6] B. A. Kemp, C. M. Bennett, and J. G. Whitney, "Efficient Estimation of Critical Transfer Belt Parameters from an Electrical Characterization Fixture", IS&T NIP **25**, 261 (2009).

[7] D. A. Hays, "Adhesion of charged particles," *Fundamentals of Adhesion and Interfaces*, 61-71 (VSP, Netherlands, 1995).
[8] J. M. Crowley, "The electrostatic problem of a dielectric sphere near a plane," IS&T NIP **24**, 299 (2008).
[9] B. A. Kemp and J. G. Whitney, "Analytical modeling of electrostatic toner adhesion," IS&T NIP **27**, 140 (2011).
[10] W. S. Czarneckia and L.B. Schein, "Electrostatic force acting on a spherically symmetric charge distribution in contact with a conductive plane," J. Electrostat. **61**, 107 (2004).
[11] B. A. Kemp and J. G. Whitney, "Electrostatic adhesion of multiple non-uniformly charged dielectric particles," J. Appl. Phys. **113**, 044903 (2013).
[12] B. A. Kemp and J. G. Whitney, "Nonlinear nature of microparticle detachment by an applied static field," Appl. Phys. Lett. **102**, 141605 (2013).
[13] J. W. Kwek, I. U. Vakarelskia, W. K. Nga, J. Y. Hengc, and R. B. Tan, "Novel parallel plate condenser for single particle electrostatic force measurements in atomic force microscope," Colloid Surface A **385**, 206 (2011).
[14] B. Techaumnat, B. Aua-arporn, and T. Takuma, Calculation of electric field and dielectrophoretic force on spherical particles in chain, J. Appl. Phys. 95, 1586 (2004).
[15] B. A. Kemp, "Resolution of the abraham-minkowski debate: Implications for the electromagnetic wave theory of light in matter," J. Appl. Phys. **109**, 111101 (2011).
[16] B. A. Kemp, T. M. Grzegorczyk, and J. A. Kong, "Optical momentum transfer to absorbing Mie particles," Phys. Rev. Lett. **97**, 133902 (2006).
[17] A. Limsimarat and B. Techaumnat, "Dynamic simulation using a multipolar model of particles under dielectrophoretic force," J. Electrostat, **65**, 672 (2007).
[18] B. A. Kemp, T. M. Grzegorczyk, and J. A. Kong, "Ab initio study of the radiation pressure on dielectric and magnetic media," Opt. Express **13**, 9280 (2005).
[19] T. M. Grzegorczyk and B. A. Kemp, "Transfer of Optical Momentum: Reconciliations of the Abraham and Minkowski Formulations," Proc. SPIE **7038**, 70381S (2008).
[20] B. A. Kemp, T. M. Grzegorczyk, and J. A. Kong, "Lorentz Force on Dielectric and Magnetic Particles," J. of Electromagn. Waves and Appl. **20**, 827 (2006).
[21] B. Techaumnat and T. Takuma, "Analysis of the electrostatic force on a dielectric particle with partial charge distribution," J. Electrostat. **67**, 686 (2009).

## Author Biography

*Brandon Kemp received his BS in Engineering from Arkansas State University (1997), MSEE from the University of Missouri-Rolla (1998), and PhD in Electrical Engineering from the Massachusetts Institute of Technology (2007). He is presently a faculty member at Arkansas State University where he won the NSF CAREER award in 2012 for his work in electrodynamics. Dr. Kemp previously spent 8 years in R&D with Lexmark.*